

# Duty-Cycle Power Manager for Thermal-Powered Wireless Sensor Networks

Trong Nhan LE\*, Alain PEGATOQUET†, Olivier SENTIEYS\*, Olivier BERDER\* and Cecile BELLEUDY†

\*IRISA/INRIA, University of Rennes 1, 6 rue de Kerampont BP 80518 - 22305 Lannion Cedex, France

†LEAT, University of Nice-Sophia Antipolis, 930 route des Colles, BP 145 - 06903 Sophia Antipolis Cedex, France

\*{trong-nhan.le, sentieys, oberder}@irisa.fr, †{alain.pegatoquet, belleudy}@unice.fr

**Abstract**—Exploiting energy from the environment to extend the system lifetime of Wireless Sensor Network (WSN), especially thermal energy, is considered as a promising approach. When considering self-powered systems, the Power Manager (PM) plays an important role in energy harvesting WSNs. Instead of minimizing the consumed energy as in the case of battery-powered systems, it causes the harvesting node to converge to Energy Neutral Operation (ENO) in order to achieve a theoretically infinite lifetime. In this paper, a low complexity PM for a thermal-powered WSN is presented. Our PM adapts the duty cycle of the node according to the estimation of harvested energy and the consumed energy provided by a simple energy monitor for a super capacitor based WSN to achieve the ENO. Experiments are performed on a real WSN platform where harvested energy is extracted from the wasted heat of a PC adapter by two thermoelectric generators.

## I. INTRODUCTION

Wireless Sensor Networks (WSN) provide a powerful combination of distributed sensing, computing and wireless communication that can be useful in various monitoring applications [1]. However, energy supply is the critical issue to meet the long-term operations in these applications. In order to design autonomous WSN, energy harvesting is considered as a promising technique. Moreover, a power manager (PM) is also embedded inside the wireless node to adapt its computation load to ensure the consumed energy is equal to harvested energy over a long period. This leads to Energy Neutral Operation (ENO) [2] with a theoretically infinite system lifetime. Most of current approaches concentrate on solar-powered WSN [2][3][4]. Not only providing the most significant energy density, solar energy is also diurnal and therefore, can be easily predicted by the PM in the near future (e.g. 30 minutes). These advantages make solar energy extracted from photovoltaic cells (PV) the most popular harvesting source [3].

In this paper, a low complexity PM for thermal-powered WSN applications is proposed. When thermoelectric generators (TEG) are employed, thermal gradients in the environment can be converted into electric energy for powering the wireless node. Even if thermal energy is often unpredictable and uncontrollable, monitoring applications based on thermal-powered WSN usually only require tracking data whenever the harvested energy from TEG is available. One example involves the monitoring of the health of industrial engines, which can exploit excess or wasted heat when they are running. Another example concerns the monitoring of patient health in a hospital

with the heat from body skin. Therefore, the PM adapts the system performance of the wireless node by changing the duty cycle to consume energy as much as it can harvest. This strategy not only maximizes the quality of service (QoS) according to the available harvested energy, but also satisfies the ENO condition. The main contributions in this paper are:

- A generic platform for thermal-powered WSN.
- An energy monitor for a super capacitor based WSN.
- A low complexity PM that only needs to read the voltage of the super capacitor to adapt the duty cycle of the wireless node.

The rest of this paper is organized as follows. In Section II, related works are presented. The architecture of the WSN using thermal energy is depicted in Section III. The energy monitor providing energy profiles is described in Section IV. The PM taking into account these profiles and performing adaptations is modeled in Section V. Experimental and simulated results are presented in Section VI. Finally, the paper ends with conclusions.

## II. RELATED WORK

The human warmth is a potential heat source for a self-powered WSN node attached to the skin. In this scenario, TEG can provide more power than PV in indoor environment as they work over day and night. A wrist-watch equipped with a TEG presented in [6] is considered as the first practical WSN application on a human body. A comparator is implemented by hardware components to control the output energy of TEG for powering the sensor node or charging a 1.2V NiMH battery. However, there is no PM implemented by software components (e.g. adaptation algorithm at the microcontroller) to control the duty cycle of the wireless node according to the available energy from TEG.

Another thermal-based WSN platform proposed in [7] can extract the heat energy from a radiator for powering a ZigBee node. Multiple storage buffers are used in their design to overcome the variation of harvested energy from a TEG and excessive power when the system starts up. Beside the charge and control circuit similar to the comparator in [6], a simple PM is implemented in the ZigBee node to reduce the hardware complexity. An overcharge and undercharge algorithm of the PM allows to enhance the lifetime of two AA rechargeable batteries. However, dynamic adaptations of the ZigBee node are missing in their approach.

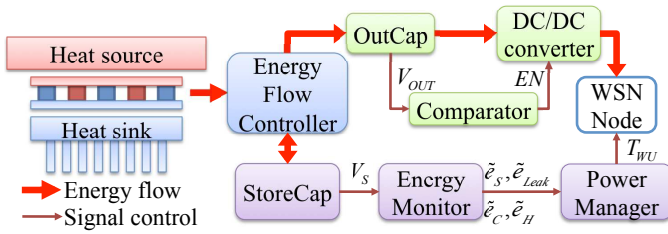


Fig. 1. Generic architecture of our thermal-powered WSN node.

In this paper, our PM is focused on adaptations of the wireless node to respect ENO condition. The wake-up period of a wireless node is mostly based on the current voltage of a super capacitor, which is used as the main storage. Characterization of the leakage energy is not required in our approach. These show the interest of our PM since it is independent of harvesters instead of only for solar cells as [12]. The PM is also low complexity and therefore, provides a practical implementation on low resources WSN.

### III. ARCHITECTURE FOR THERMAL-POWERED WSN

The architecture of our WSN using thermal energy is depicted in Fig. 1. The hot surface of the TEG is attached to a heat source while the cold surface is commonly chosen to provide the heat spreading effect towards a heat sink. The different temperatures between two surfaces result in an output voltage by the Seebeck effect and hence, generates thermal energy. This energy is then distributed by an energy flow controller to two capacitors OutCap and StoreCap, which have different charging priority as proposed in [8]. This structure not only takes advantage of the virtual recharge cycle of capacitors compared to batteries to prolong system lifetime, but also enables robust booting from the exhausting energy of the system.

Firstly, the harvested energy is used to charge OutCap, which has the highest charging priority and relative small capacitance compared to StoreCap. Due to the small capacitance, its voltage ( $V_{OUT}$ ) is rapidly increased to a rising threshold and then, a comparator, implemented by hardware components, enables a DC/DC converter for powering the wireless node. As soon as  $V_{OUT}$  reaches the regulation level ( $V_{Re}$ ), the StoreCap is allowed to be charged. Whenever  $V_{OUT}$  drops under  $V_{Re}$ , energy from both TEG and StoreCap will charge the OutCap.

The PM is considered as the core of the energy harvesting WSN node. It is implemented by software components and embedded inside the microcontroller of the wireless node. The main goal of the PM is to operate the WSN node in ENO, which means the harvested energy is equal to the consumed energy over a long period. For a thermal-powered WSN, the PM tries to keep the voltage of the StoreCap ( $V_S$ ) almost constant and therefore, the equality of harvested and consumed energy is respected. According to the estimation of the harvested energy ( $\tilde{e}_H$ ) as well as the consumed energy ( $\tilde{e}_C$ ) provided by the energy monitor, the PM adapts the application QoS by determining the next wake-up period of the node

( $T_{WU}$ ) to respect the ENO constraint.

### IV. SUPER CAPACITOR BASED ENERGY MONITOR

In this section, a simple energy monitor for a super capacitor based WSN is proposed. It is embedded in the energy harvesting WSN to provide various energy profiles, including stored energy, harvested energy and consumed energy. The time domain is divided into slots of duration  $T_S(n)$  and the energy monitor is carried out at the end of each slot. By reading the current voltage of StoreCap ( $V_S$ ) and looking up a table characterizing consumed energy of atomic functions, the following discrete energy values are evaluated:

- $\tilde{e}_S(n)$ ,  $\tilde{e}_{Leak}(n)$ : available energy in StoreCap at the end of slot  $n$  and leakage energy of the whole system during slot  $n$ , provided by the stored energy model.
- $\tilde{e}_C(n)$ : consumed energy of the wireless node during slot  $n$ , provided by the consumed energy model.
- $\tilde{e}_H(n)$ : harvested energy during slot  $n$ , provided by the harvested energy model.

#### A. Stored energy model

The available energy in the StoreCap at the end of slot  $n$  can be approximated according to its voltage  $V_S(n)$  and capacitance  $C_S$  as

$$\tilde{e}_S(n) = \frac{1}{2} C_S V_S(n)^2. \quad (1)$$

Meanwhile, the leakage energy of the whole system during slot  $n$  depends on  $C_S$ . As shown in [5], leakage energy is more severe for larger capacitor than for smaller one. However, for a specified  $C_S$ , leakage energy can be estimated by

$$\tilde{e}_{Leak}(n) = P_{Leak} T_S(n), \quad (2)$$

where  $P_{Leak}$  is the leakage power, which is considered as a constant.

#### B. Consumed energy model

In a WSN application, a node periodically wakes up and briefly turns on active mode for sensing and RF communication. It stays most of the time in sleeping mode for energy reservation. Therefore, the total consumed energy during slot  $n$  can be divided into two parts as

$$\tilde{e}_C(n) = \tilde{e}_{Active}(n) + \tilde{e}_{Sleep}(n),$$

where  $\tilde{e}_{Active}(n)$  is the consumed energy in active time and  $\tilde{e}_{Sleep}(n)$  is the consumed energy in sleeping time. As the consumed current is nearly constant in sleep mode,  $\tilde{e}_{Sleep}(n)$  can be easily estimated based on the sleep power  $P_{Sleep}$  as

$$\tilde{e}_{Sleep}(n) = P_{Sleep} T_{Sleep}(n) \approx P_{Sleep} T_S(n) \quad (3)$$

The total sleeping time during slot  $n$  ( $T_{Sleep}(n)$ ) is approximated to  $T_S(n)$  as the total active time is negligible (in order of  $ms$ ) compared to the sleeping time (in order of  $s$ ). However, it is more complex to estimate  $\tilde{e}_{Active}(n)$  based on the power as many different scenarios in the active time results in a variation of the consumed current of the WSN node. Therefore, to obtain

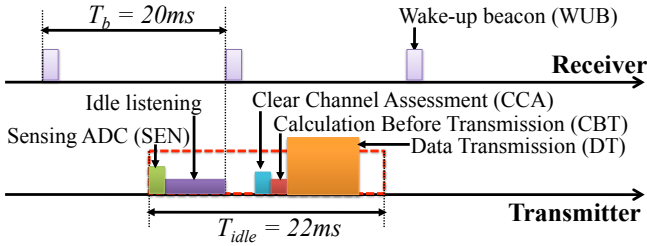


Fig. 2. Communication between two nodes following our model.

more accurate measurements, it is necessary to identify the consumed energy of many scenarios according to a specific WSN platform.

In this paper, the PowWow [10] platform, which is based on the MSP430 microcontroller and the CC2420 RF transceiver, is used. Two PowWow nodes perform communication based on the RICER MAC protocol [11] shown in Fig. 2. The receiver, powered by batteries and connected to a host computer, sends a wake-up beacon (WUB) each  $T_b = 20ms$ . When waking up, the transmitter reads a value from its sensor through an ADC channel (SEN) and then, waits for a WUB from the receiver (idle listening). Once a WUB is received, the transmitter performs Clear Channel Assessment (CCA) and Calculation Before Transmission (CBT) before transmitting a data packet (DT). In order to deal with clock drift, the maximum idle listening time at transmitter is set to 22ms. The consumed energy for these activities on PowWow platform have been already characterized and gathered into a look-up table [9]. The microcontroller keeps tracking all activities of the node to estimate the consumed energy in active mode during a slot. We define  $k$  as the number of wake-up times occurring during slot  $n$ . Therefore, the total consumed energy in active period can be expressed as

$$\begin{aligned} \tilde{e}_{Active}(n) &= \sum_{i=1}^k t_{idle}(i) P_{Rx} \\ &+ k(E_{SEN} + E_{WUB} + E_{CCA} + E_{CBT} + E_{DT}) \end{aligned} \quad (4)$$

where  $t_{idle}(i) \in [0, 22]$  is the  $i^{th}$  idle listening time. Finally, the total consumed energy during slot  $n$  is estimated as

$$\tilde{e}_C(n) = \tilde{e}_{Active}(n) + P_{Sleep} T_S(n) \quad (5)$$

### C. Harvested energy model

Following the energy flow principles explained in Section III, the harvested energy is distributed into three parts after the energy flow controller (Fig. 1). The first part is directly consumed by the DC/DC converter to power the wireless node. The second one is stored into the StoreCap and the final one is consumed by the leakage energy. Therefore, the harvested energy during slot  $n$  can be estimated by

$$\tilde{e}_H(n) = \frac{1}{\eta} \tilde{e}_C(n) + [\tilde{e}_S(n) - \tilde{e}_S(n-1)] + \tilde{e}_{Leak}(n) \quad (6)$$

where  $\eta$  is the DC/DC converter efficiency,  $\tilde{e}_C(n)$  is the consumed energy of the wireless node,  $[\tilde{e}_S(n) - \tilde{e}_S(n-1)]$  is the energy stored in the StoreCap during the slot  $n$  and  $\tilde{e}_{Leak}$  is the leakage energy. When the harvested energy is greater

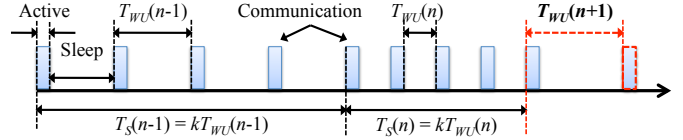


Fig. 3. Power manager with dynamic adaptation period.

than the sum of the consumed energy and the leakage energy, a part of harvested energy is consumed by the wireless node and leakage and therefore, only the surplus harvested energy will charge the StoreCap. On the other hand, when the harvested energy is less than the sum of the consumed energy and the leakage energy, all harvested energy is transferred to the load and the remaining energy is served by the StoreCap. In this case, the first term in (6),  $[\tilde{e}_S(n) - \tilde{e}_S(n-1)]$ , is negative.

Using energy profiles presented in this section, the PM is able to adapt the wake-up period of the node in order to respect the ENO. Our PM approach is explained in the next section.

## V. POWER MANAGER WITH DYNAMIC ADAPTATION PERIOD

In this section, a PM for a periodic monitoring application shown in Fig. 3 is proposed. We defined  $V_{Ref}$  is the desired voltage of the StoreCap when the node has converged to ENO. The PM estimates the wake-up period ( $T_{WU}$ ) to respect the ENO in the next slot and keep  $V_S$  around  $V_{Ref}$ . Whenever the node wakes up,  $V_S$  is read by a low power ADC (SEN) and, is integrated in a packet and sent to a receiver using the protocol shown in Fig. 2. After a predefined number of wake-up times ( $k$ ), the PM is activated to estimate the next  $T_{WU}$ . Therefore, the adaptation period of the PM is

$$T_S(n) = kT_{WU}(n) \quad (7)$$

This dynamic period as shown in [12], provides a way to adapt the reactivity of the PM according to the current  $T_{WU}(n)$ .

At the end of slot  $n$ , the energy monitor is activated to provide the energy profiles, including the consumed energy  $\tilde{e}_C(n)$  and the harvested energy  $\tilde{e}_H(n)$ . Based on these profiles, the PM predicts the consumed energy  $\hat{e}_C(n+1)$  and the harvested energy  $\hat{e}_H(n+1)$  for the next slot ( $n+1$ ). Firstly,  $\hat{e}_C(n+1)$  can be predicted as

$$\hat{e}_C(n+1) = \hat{e}_{Active}(n+1) + P_{Sleep} k T_{WU}(n+1) \quad (8)$$

where  $\hat{e}_{Active}(n+1)$  is the predicted energy during active period and  $P_{Sleep} k T_{WU}(n+1)$  stands for sleep energy in slot ( $n+1$ ). As the node has the same  $k$  wake-up times every slot,  $\hat{e}_{Active}(n+1)$  can be predicted using the Exponentially Weighted Moving Average filter (EWMA) [2] :

$$\hat{e}_{Active}(n+1) = \alpha \hat{e}_{Active}(n) + (1 - \alpha) \tilde{e}_{Active}(n) \quad (9)$$

where  $\alpha \in [0, 1]$  is a weighted factor. Since the variation of  $\tilde{e}_{Active}(n)$  (due to different  $\sum_{i=1}^k t_{idle}(i)$  in (4)),  $\alpha$  should be greater than 0.5 to reduce the contribution of the recent value  $\tilde{e}_{Active}(n)$ . This strategy makes  $\hat{e}_{Active}(n+1)$  converge to the average energy for  $k$  communications in a slot.

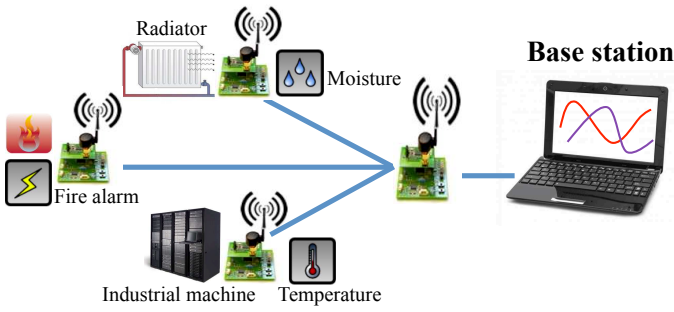


Fig. 4. A monitoring application based on thermal-powered WSN.

In order to predict the harvested energy from TEG, it is assumed that the harvested power ( $\tilde{P}_H$ ) is the same during two consecutive slots as the slow change of the heat energy. Therefore,

$$\hat{e}_H(n+1) = \tilde{P}_H(n)T_S(n+1) = \tilde{P}_H(n)kT_{WU}(n+1) \quad (10)$$

Moreover, the residual energy at the end of slot  $n$ , which is the energy difference between the current state and desired state (when  $V_S = V_{Ref}$ ) or the error energy due to prediction methods of the slot  $n-1$ , can be considered as the additional budget energy for the next slot and is defined as following:

$$\tilde{e}_{Bud}(n) = \tilde{e}_S(n) - \frac{1}{2}C_S V_{Ref}^2 = \frac{1}{2}C_S (V_S^2(n) - V_{Ref}^2) \quad (11)$$

Therefore, to satisfy the ENO condition in the slot  $(n+1)$ , the following constraint needs to be respected:

$$\hat{e}_H(n+1) - \tilde{e}_{Leak}(n+1) + \tilde{e}_{Bud}(n) = \frac{1}{\eta} \hat{e}_C(n+1) \quad (12)$$

By applying (8) and (10) into (12), the next wake-up period can be determined as follows

$$T_{WU}(n+1) = \frac{[\hat{e}_{Active}(n+1) - \eta \tilde{e}_{Bud}(n)]/k}{\eta(\tilde{P}_H(n) - P_{Leak}) - P_{Sleep}} \quad (13)$$

Moreover, by dividing both sides of (6) by  $T_S(n)$ , we have

$$\tilde{P}_H(n) = \frac{\tilde{e}_{Active}(n)}{\eta T_S(n)} + \frac{P_{Sleep}}{\eta} + \frac{\tilde{e}_S(n) - \tilde{e}_S(n-1)}{T_S(n)} + P_{Leak}$$

By moving  $P_{Sleep}/\eta$  and  $P_{Leak}$  to the left and replacing this result to the denominator of (13), we achieve

$$T_{WU}(n+1) = \frac{[\hat{e}_{Active}(n+1) - \eta \tilde{e}_{Bud}(n)] T_{WU}(n)}{\eta [\tilde{e}_S(n) - \tilde{e}_S(n-1)] + \tilde{e}_{Active}(n)} \quad (14)$$

This result shows the simple implementation of the PM. At the beginning of the next slot, the PM only needs to read the voltage of the StoreCap ( $V_S(n)$ ) and based on the consumed energy in previous slot ( $\tilde{e}_{Active}(n)$ ), the next wake-up period is computed. However, the PM can provide an invalid  $T_{WU}$  due to the noise when reading  $V_S$  through the ADC channel of the wireless node. To reduce this problem, three samples of  $V_S$  are read when the PM is activated and, an average value  $\bar{V}_S$  is used to evaluate the next wake-up period.

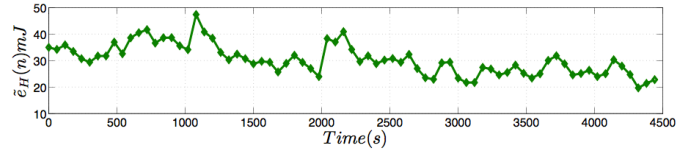


Fig. 5. Thermal energy profile extracted from a real PowWow node.

 TABLE I  
 COMPARISON OF DIFFERENT VALUES OF  $k$ 

$k$	$T_{WU}(s)$				$V_S(mV)$				Total packets
	Min	Max	Mean	Var	Min	Max	Mean	Var	
5	1	6	2.64	1.95	4000	4132	4092	654	1675
10	1	6	2.64	1.70	4000	4141	4091	740	1685
15	1	6	2.65	1.64	4000	4194	4114	728	1690
20	1	5	2.67	1.34	4000	4315	4229	2135	1691

## VI. EXPERIMENTAL RESULTS

Our experiments are performed using PowWow platforms to illustrate the monitoring application shown in Fig. 4. The transmitter sends its packets to a receiver, which is connected to a host PC, by the protocol depicted in Fig. 2. The transmitter is equipped by two TEG connected in parallel. Their hot surfaces are attached to a laptop adapter as the heat source while cold surfaces are chosen to provide the heat spreading effect towards the heat sinks. The temperature gradient between the working PC adapter and the ambient air provides around 50mV output by two TEGs. The LTC3108 component is used as an energy flow controller to drive harvested energy from TEG. It provides a complete solution for energy harvesting WSN with two outputs. The first output is connected to the OutCap for powering the PowWow node, while the second one is connected to the StoreCap for energy storage. The low energy ADC of MSP430 is used to read  $V_S$ .

Firstly, harvested energy profile extracted from a real PowWow node is used as the input of a simulation program to determine the  $k$  parameter in (7), which represents the reactivity of the PM. As it is observed in Fig. 5, harvested energy has high fluctuations since the Maximum Power Point Tracking is not implemented in the PowWow platform. Therefore, energy from TEG is extracted at random power point. Moreover, the harvested energy model suffers the errors of the energy monitor when reading  $V_S$ . Simulation results with  $C_S = 0.09F$ ,  $V_S = 4V$  at the beginning and  $\alpha = 0.6$  are summarized in Table I. As the resolution of  $T_{WU}$  is in second, (14) is modified by a round function to return the nearest integer number. When  $k = 5$ , the PM has a fast response to the harvested energy. This value causes the biggest variation of  $T_{WU}$  but the lowest variation of  $V_S$ . In this case,  $T_{WU}$  is more regularly updated by the PM and therefore,  $V_S$  is more stable compared to higher values of  $k$ . When  $k$  is increased, the variation of  $T_{WU}$  is reduced but  $V_S$  can move far from the ENO state as the PM has a slow response. From Table I, the lowest variation of  $T_{WU}$  but the highest variation of  $V_S$  is when  $k = 20$ . It is worth noting that, due to overhead computations of the PM, the total number

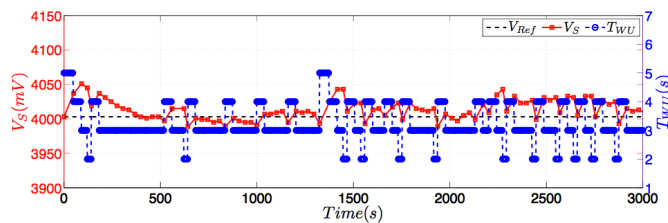


Fig. 6. Power manager performs adaptation on a real PowWow node.  $\bar{V}_S$  is kept almost constant around  $V_{Ref}$ , which represents the ENO condition.

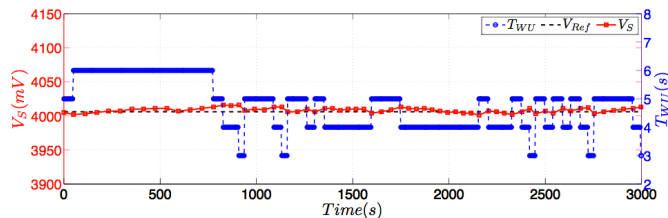


Fig. 7. Voltage of the StoreCap and wake-up period of the PowWow node when a new super capacitor 0.18F is used.

of transmitted packets is reduced when  $k = 5$ . However, this effect is minor as the consumed energy by the PM, estimated as  $E_{PM} = 3E_{SEN}$  ( $E_{SEN}$  represents the required energy for sampling  $V_S$ ), is negligible compared to the energy for wireless communications during a slot. When  $k = 10$ ,  $E_{PM}$  represents only 0.9% of  $\tilde{e}_C(n)$ . Therefore, the choice of  $k$  is only required to balance the variation of  $T_{WU}$  and  $V_S$ . For the next experiments,  $k = 10$  is used in this section.

Secondly, the PM is implemented on the transmitter node with the same configuration as the simulation program ( $C_S = 0.09F$  and  $\alpha = 0.6$ ). Fig. 6 presents the adaptation of  $T_{WU}$  according to the change of  $\bar{V}_S$ . At the beginning of the experiment, the default  $T_{WU}$  is set to 5s. As  $k = 10$ , the PM performs the first adaptation after 50s and  $T_{WU}$  is reduced to 4s and next 40s,  $T_{WU} = 3s$  as  $\bar{V}_S$  is increasing. In the next 30s,  $\bar{V}_S$  is lightly decreased, but  $T_{WU}$  is kept reducing to 2s as  $\bar{V}_S$  is higher than  $V_{Ref}$ . The budget energy now is positive and therefore, the numerator in (14) is significantly reduced. After that,  $T_{WU}$  is kept in 3s as long as the PM detects a considerable drop of  $\bar{V}_S$ . During the experiment,  $\bar{V}_S$  is kept in almost constant around  $V_{Ref}$ . It means that our PM is able to match the harvested and consumed energy over a long period and keep the PowWow node running in ENO.

The biggest advantage of our PM is the independence of leakage energy, which is a non-negligible consumed energy in a super capacitor based WSN. As it can be observed in (14), characterization of the leakage energy is not required for adaptations of the PM. Fig. 7 presents the voltage of the StoreCap and the wake-up period of the wireless node when two 0.09F capacitors are connected in parallel ( $C_S = 0.18F$ ). As the leakage energy increases, the average  $T_{WU}$  is also higher than experiment presented in Fig. 6. At the first 750s,  $T_{WU}$  converges to 6s. However, in the next 2000s, there seems to be more heat from TEG and  $T_{WU}$  is around 4s. Moreover, due to bigger capacitance,  $\bar{V}_S$  is more stable than

in case of Fig. 6. This behavior is useful for monitoring the health of industrial engines by exploiting the wasted heat when they are running. By real time tracking data including temperature, vibration and pressure, a great deal of time and money can be saved since regular engine maintenance will not be required until the analyzed data shows it is necessary. Real time detection and diagnosis of patient disease is also a promising application for our PM.

## VII. CONCLUSION

The power manager is considered as the critical component in self-powered WSNs to match the harvested energy and the consumed energy over a long period. In this paper, a low complexity PM for a super capacitor based thermal-powered WSN provides practical adaptations to respect the ENO constraint in energy harvesting WSN. Experiments show that the PowWow node with our PM is able to keep the harvested and consumed energy in equilibrium to extend the system lifetime. This behavior is suitable for long-term monitoring applications where the wasted ambient heat can be found most of the time. The adaptations mostly based on the voltage of the StoreCap makes our PM independent of harvesters and therefore, can be extended to other energy sources such as wind and vibration energy. Moreover, multihop scenarios will be considered in future works.

## REFERENCES

- [1] D. Puccinelli and M. Haenggi, "Wireless sensor networks: applications and challenges of ubiquitous sensing," *Circuits and Systems Magazine, IEEE*, vol. 5, no. 3, pp. 19 – 31, 2005.
- [2] J. Hsu, S. Zahedi, A. Kansal, M. Srivastava, and V. Raghunathan, "Adaptive duty cycling for energy harvesting systems," in *Proceedings of the International Symposium on Low Power Electronics and Design (ISLPED)*, pp. 180–185, 2006.
- [3] C. Moser, L. Thiele, D. Brunelli, and L. Benini, "Adaptive power management in energy harvesting systems," in *Design, Automation Test in Europe (DATE)*, pp. 1–6, 2007.
- [4] C. Vigorito, D. Ganesan, and A. Barto, "Adaptive control of duty cycling in energy-harvesting wireless sensor networks," in *IEEE Communications Society Conference on Sensor, Mesh and Ad Hoc Communications and Networks (SECON)*, pp. 21–30, 2007.
- [5] T. Zhu, Z. Zhong, Y. Gu, T. He, and Z. Zhang, "Leakage-aware energy synchronization for wireless sensor networks," in *International Conference on Mobile systems, applications, and services*, pp. 319–332, 2009.
- [6] V. Leonov, T. Torfs, P. Fiorini, and C. Van Hoof, "Thermoelectric converters of human warmth for self-powered wireless sensor nodes," *Sensors Journal, IEEE*, vol. 7, no. 5, pp. 650–657, 2007.
- [7] X. Lu and S.-H. Yang, "Thermal energy harvesting for wsn," in *Systems Man and Cybernetics (SMC), 2010 IEEE International Conference on*, pp. 3045–3052, 2010.
- [8] C.-Y. Chen and P. H. Chou, "Duracap: a supercapacitor-based, power-bootstrapping, maximum power point tracking energy-harvesting system," in *Proceedings of International Symposium on Low Power Electronics and Design (ISLPED)*, pp. 313–318, 2010.
- [9] M.M. Alam, O. Berder, D. Menard, T. Anger, and O. Sentieys, "A hybrid model for accurate energy analysis of wsn nodes," *Journal on Embedded Systems (EURASIP)*, vol. 2011, p. 16, 2011.
- [10] [Online]. Available: <http://powwow.gforge.inria.fr>
- [11] E.-Y. Lin, J. Rabaey, and A. Wolisz, "Power-efficient rendez-vous schemes for dense wireless sensor networks," in *IEEE International Conference on Communications*, vol. 7, pp. 3769 – 3776, 2004.
- [12] A. Castagnetti, A. Pegatoquet, C. Belleudy, and M. Auguin, "A framework for modeling and simulating energy harvesting wsn nodes with efficient power management policies," *EURASIP Journal on Embedded Systems*, 2012.